

# Maximum Power Point Tracking With Fractional Order High Pass Filter for Proton Exchange Membrane Fuel Cell

Jianxin Liu, Tiebiao Zhao, and YangQuan Chen

**Abstract**—Proton exchange membrane fuel cell (PEMFC) is widely recognized as a potentially renewable and green energy source based on hydrogen. Maximum power point tracking (MPPT) is one of the most important working conditions to be considered. In order to improve the performance such as convergence and robustness under disturbance and uncertainty, a fractional order high pass filter (FOHPF) is applied for the MPPT controller design based on the traditional extremum seeking control (ESC). The controller is designed with integer-order integrator (IO-I) and low pass filter (IO-LPF) together with fractional order high pass filter (FOHPF), by substituting the normal HPF in the original ESC system. With this FOHPF ESC, better convergence and smoother performance are achieved while maintaining the robust specifications. First, tracking stability is discussed under the commensurate-order condition. Then, simulation results are included to validate the proposed new FOHPF ESC scheme under disturbance. Finally, comparison results between FOHPF ESC and the traditional ESC method are also provided.

**Index Terms**—Extremum seeking control (ESC), fractional order high pass filter (FOHPF), fuel cell, fractional controller stability, maximum power point tracking (MPPT).

## I. INTRODUCTION

**P**ROBLEMS about energy crisis and environment pollution related to fossil fuel are intensively studied all over the world [1]–[3]. Energy saving and looking for new-generation reproductive energy source are considered helpful for attenuating these problems. Nuclear energy, solar cell, wind, fuel cell, and hydro power are alternative green power sources [4],[5]. Recently, the fuel cell (FC) has gained attention as a new power source because of higher energy density than fossil fuels. Moreover, the FC is eco-friendly because only water and heat are produced as by-products [6]. Hydrogen fuel cell is a kind of power source to gain electric power from chemical one under control, which is considered as an emerging renewable green power source. However, due

to its low reaction rate and difficulty of hydrogen availability, many different fuel cell types have been tried, such as alkaline (AFC), proton exchange membrane (PEMFC), direct methanol (DMFC), phosphoric acid (PAFC), molten carbonate (MCFC), solid oxide (SOFC) [7]. Among various types of FC, the PEMFC is suitable for some special applications such as unmanned aerial vehicles (UAVs) because of high loading capability due to relatively lighter weight, and ease of miniaturization, low operating temperature at which ion conductivity is adequate to generate high power and use of solid-state electrolyte.

Since the cost of PEMFC is a little expensive now, so, in many cases, efficiency must be the most important factor taken into consideration when designing a PEMFC and the related controller. However, sometimes, how to extract the maximum power fast and stably should be placed on the first position. For a typical application scenario, a working UAV should have four stages: taking-off, climbing, cruising and landing, as shown in Fig. 1. It is well known that taking off and landing will draw more power from the energy system, requiring the FC system to work at maximum power point [8]. However, it is also known that the power output of PEMFC is dependent not only on internal chemical reaction but also on external load impedance [9]. And the operating point is the intersection of PEMFC's characteristic P-I curve and the load line, as shown in Fig. 2. If the current drawn from the cell is tuned to the maximum power point with value of  $I^*$ , then the cell works under the maximum power point  $P^*$  which is an equilibrium

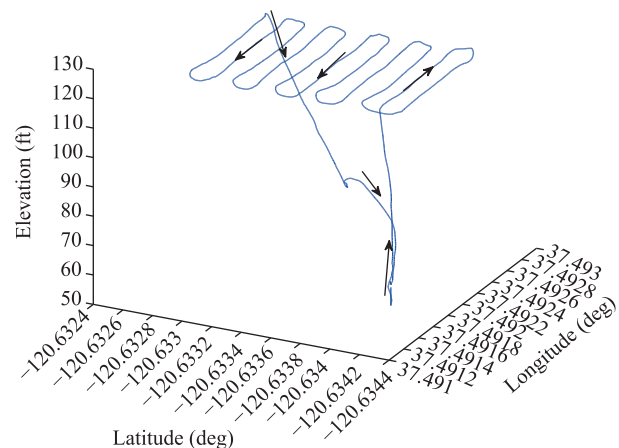


Fig. 1. Drone trajectory as an example during implementing a task.

Manuscript received September 1, 2015; accepted February 28, 2016. This work was supported by the Research Project Granted by Xihua University. Recommended by Associate Editor Dingyü Xue.

Citation: J. X. Liu, T. B. Zhao, and Y. Q. Chen, "Maximum power point tracking with fractional order high pass filter for proton exchange membrane fuel cell," *IEEE/CAA Journal of Automatica Sinica*, vol. 4, no. 1, pp. 70–79, Jan. 2017.

J. X. Liu is with the School of Mechanical Engineering, Xihua University, Chengdu 610039, China (e-mail: jamson\_liu@163.com).

T. B. Zhao and Y. Q. Chen are with University of California, Merced, CA95343, USA (e-mail: tzhao@ucmerced.edu; ychen53@ucmerced.edu).

Color versions of one or more of the figures in this paper are available online at <http://ieeexplore.ieee.org>.

Digital Object Identifier 10.1109/JAS.2017.7510328

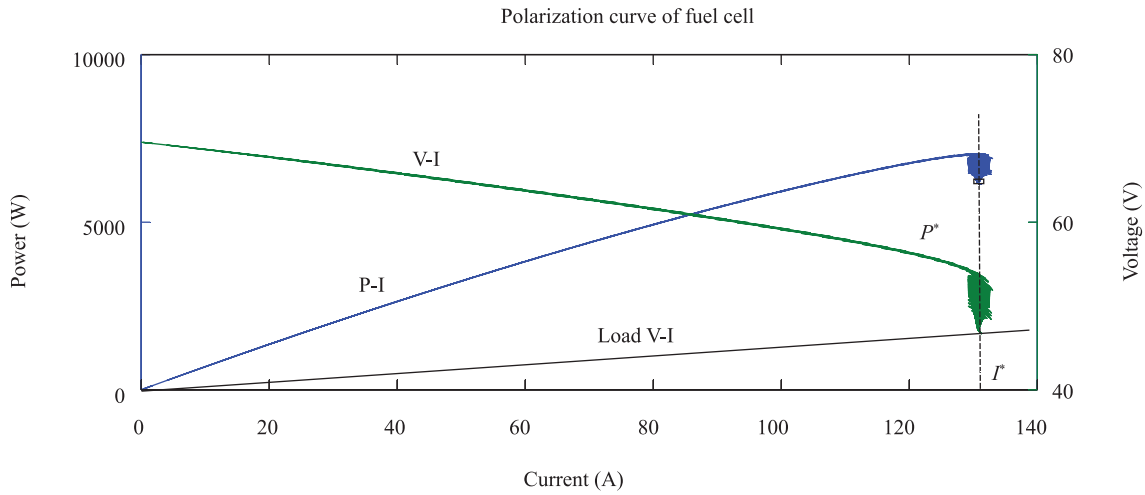


Fig. 2. Typical polarization curve and the maximum power point.

point. It is worthy to point out that the polarization curve is nonlinear and time-variant. So the setpoint is inclined to shift when the working parameters are changed, and the MPPT for PEMFC is in fact a dynamic optimization problem thus control schemes with capability of more robustness via adaptation are needed.

The problem of extracting the maximum power from renewable energy sources was first done for processes like photovoltaic panels (PV) and wind turbines [10]. Up to now, extensive research work has been done on photovoltaic power applications, such as the perturbation and observe (P&O) method, the conductance incremental method, the parasitic capacitance method, the short current method, model-based methods, and artificial intelligence methods. But relatively few researches on fuel cell MPPT control have been reported. Among them the P&O algorithm is by far the most commonly used in practice because of its ease of implementation [11]. However, due to the limitation that P&O exhibits erratic and unstable behavior under rapidly changing environments, thus the algorithm is unsuitable for the job of tracking the frequently moving MPP.

Extremum seeking is an adaptive nonlinear control method which has been used since 1950s, but its theoretical foundations for its stability and performance were established very late by [12]. Yin *et al.* discussed a class of nonlinear systems controlled by fractional order slide-mode extremum seeking control strategy and succeeded in lighting control applications [13], [14]. Bizon applied an ESC scheme to PEMFC, by setting the dither amplitude to be proportional with the magnitude of first harmonics of the processed FC power [15]. Fig.3 is the simplest peak searching scheme. The higher order extremum seeking (hoES) control scheme is based on the classical control extremum seeking scheme, which is augmented with a low pass filter (LPF) and/or a high pass filter (HPF), as shown in Fig. 4. Usually, the HPF is used to eliminate the slowly changing DC component from the signal  $P$  which is demodulated by multiplication with sinusoidal signals. The integrator could attenuate the high-frequency periodical signal around zero. Finally, the gradient of the output power is calculated.

In Fig.4, if  $P$  is the output power of the controlled fuel cell with current  $I$ , the DC component of  $P$  is attenuated by high pass filter (HPF) and the left component will be in phase or out of phase with the perturbation signal if the current is less than or greater than the optimum value. So, after being modulated using the multiplication operation, the DC component extracted by the low pass filter (LPF) is greater or less than zero. Finally, the gradient of  $I$  is used to force the power to converge to the maximum point.

So far, different algorithms have been proposed for fuel cell MPP tracking. Zhong *et al.*, reported a first attempt to track MPP by an extremum seeking algorithm [9]. Bizon proposed an architecture of hybrid power source for vehicle application operating at MPP of the fuel cell using extremum seeking [15]. Dargahi *et al.* proposed MPP tracking for fuel cell in fuel cell/battery hybrid power systems using perturbation and observe (P&O) algorithm [16].

The main contribution of this work lies in two aspects. One is discussing the influence of fractional order integrator and high pass filter (HPF) on the stability of maximum power point tracking (MPPT) based on extremum seeking control (ESC). Another one is demonstrating the response smoothness of ESC with fractional order HPF (FOHPF) when applied to PEMFC. The objective is to improve PEMFC performance and robustness under disturbance, through a fractional order control scheme instead of an integer order one.

The paper is organized as follows. The preliminaries of stability of fractional order transfer functions are discussed

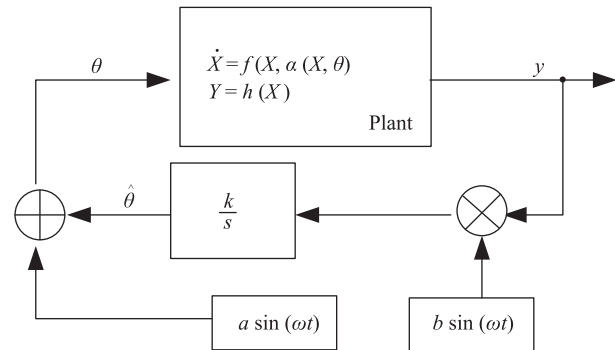


Fig. 3. The simplest peak searching scheme.

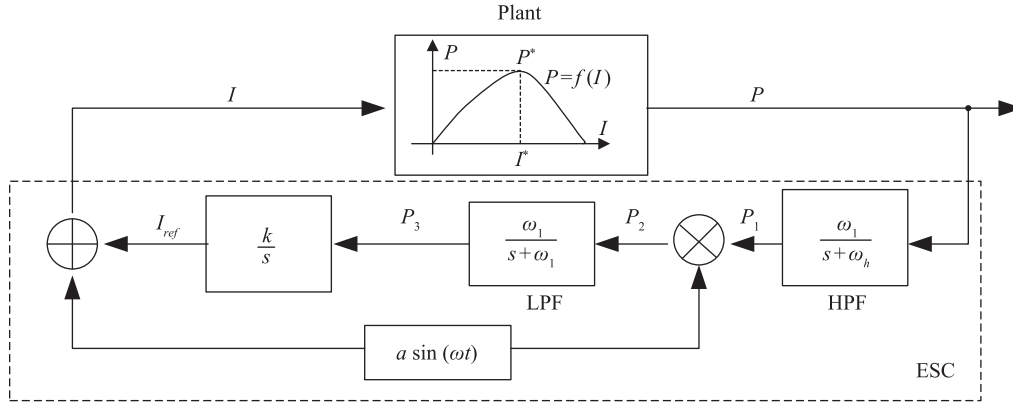


Fig. 4. General ESC control scheme.

in Section II; and in Section III, an adaptive MPPT controller is designed. In Section IV extremum seeking is applied to the fuel cell power system and simulation results are discussed in detail.

## II. STABILITY OF FRACTIONAL ORDER TRANSFER FUNCTION (TF)

Usually, linear time invariant (LTI) fractional order (FO) system can be described by fractional order differential equation (FODE) of the form

$$(a_n D^{\alpha_n} + a_{n-1} D^{\alpha_{n-1}} + \dots + a_1 D^{\alpha_1} + a_0) y(t) = (b_m D^{\beta_m} + b_{m-1} D^{\beta_{m-1}} + \dots + b_1 D^{\beta_1} + b_0) x(t) \quad (1)$$

where  $D^\gamma = {}_0 D_t^\gamma$ ;  $y(t)$  and  $x(t)$  represent the system output and input signals, respectively;  $a_i$  ( $i = 0, \dots, n$ ) and  $b_j$  ( $j = 0, \dots, m$ ) are constants;  $\alpha_i$  ( $i = 0, \dots, n$ ) and  $\beta_j$  ( $j = 0, \dots, m$ ) are arbitrary real numbers.

Under zero initial conditions, the transfer function of fractional order systems can be obtained as

$$G(s) = \frac{Y(s)}{X(s)} = \frac{b_m s^{\beta_m} + b_{m-1} s^{\beta_{m-1}} + \dots + b_1 s^{\beta_1} + b_0}{a_n s^{\alpha_n} + a_{n-1} s^{\alpha_{n-1}} + \dots + a_1 s^{\alpha_1} + a_0} = \frac{Num(s)}{Den(s)} \quad (2)$$

Provided that  $s^{1/\nu}$  is the greatest common factor of  $Num(s)$  and  $Den(s)$ ,  $G(s)$  can be transformed to integer order transfer function in  $w$ -domain with  $w = s^{1/\nu}$ , which is the so called commensurate-order system.

With this transformation, the Riemann surface consists of Riemann sheets and the principal Riemann sheet (PRS) located in the area

$$-\frac{\pi}{\nu} < \arg(w) < \frac{\pi}{\nu} \quad (3)$$

The stability condition is expressed as:

$$|\arg(w_i)| > \frac{1}{\nu} \cdot \frac{\pi}{2} \quad (4)$$

where  $w_i$  is the root of the characteristic polynomial in  $w$ -domain.

## III. DESIGN AND STABILITY ANALYSIS OF MPPT CONTROLLER BASED ON ESC

### A. Fractional Order Average Linear Model

The averaged linearized model relating the optimized point and the error signal for integer order ESC (IO-ESC) in Fig. 4 is [17]:

$$\frac{\tilde{\theta}}{\theta^*} = \frac{1}{1 + L(s)} \quad (5)$$

where

$$L(s) = \frac{ka^2}{2s} \left( \frac{s + j\omega}{s + j\omega + \omega_h} + \frac{s - j\omega}{s - j\omega + \omega_h} \right) \quad (6)$$

So,

$$\begin{aligned} \frac{\tilde{\theta}}{\theta^*} &= \frac{1}{1 + L(s)} \\ &= \frac{s(s^2 + 2\omega_h s + \omega_h^2 + \omega^2)}{s^3 + (2\omega_h + ka^2)s^2 + (\omega_h^2 + \omega^2 + ka^2\omega_h)s + ka^2\omega^2} \end{aligned} \quad (7)$$

By replacing  $s$  with  $s^q$ , Malek deduced the averaged linearized model for the FO-ESC as shown in Fig. 5 [18]:

$$\begin{aligned} \frac{\tilde{\theta}}{\theta^*} &= \frac{1}{1 + L(\lambda)} \\ &= \frac{\lambda(\lambda^2 + 2\omega_h \lambda + \omega_h^2 + \omega^2)}{\lambda^3 + (2\omega_h + ka^2)\lambda^2 + (\omega_h^2 + \omega^2 + ka^2\omega_h)\lambda + ka^2\omega^2} \end{aligned} \quad (8)$$

where  $\lambda = s^q$ .

When  $ka^2$  is small relative to  $\omega$ , the IO-ESC transfer function is asymptotically stable for all  $k > 0$ , with a pair of closed-loop poles making the system lightly damped. On the other hand, in the FO-ESC model, there is no pole close to the stability boundaries. However, the problem of stability in the cases of the integrator, LPF and HPF with different order value  $q$  for  $s^q$  is necessary to be discussed further. Combinations of integrator, LPF, HPF with or without fractional order operation are also valuable to discuss. Without loss of generality, the case considering only an integrator or a HPF utilizing fractional order operation without a low-pass filter (LPF) will be discussed first, as shown in Fig. 6.

### B. FO-ESC Model With Different Fractional Order of Integrator and HPF

In Fig. 6, the ESC system can be modeled as:

$$P(t) = f^*(t) + (\theta(t) - \theta^*(t)) \quad (9)$$

$$\theta_0(t) = a \sin(\omega t), \quad (10)$$

$$\theta(t) = \theta_0(t) + \frac{k}{s^\alpha} [P_3(t)] \quad (11)$$

$$\tilde{\theta}(t) = \theta^* - \theta(t) + \theta_0(t) \quad (12)$$

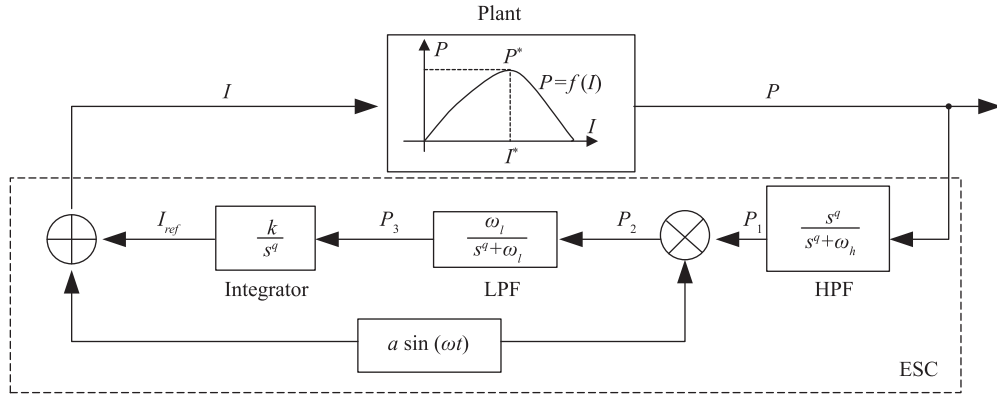


Fig. 5. Fractional order ESC (FO-ESC) control scheme.

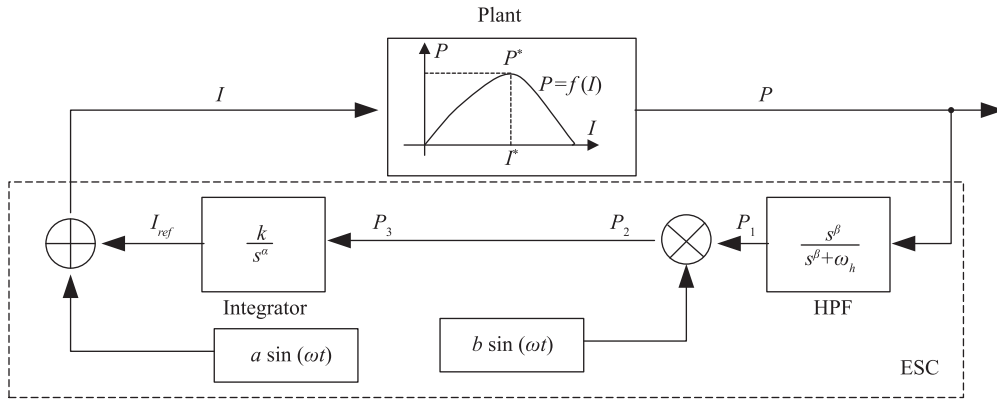


Fig. 6. Fractional order ESC (FO-ESC) without LPF.

$$P_3(t) = b \sin(\omega t) \frac{s^\beta}{s^\beta + \omega_h} [P(t)] \quad (13)$$

where  $G(s)[u(t)]$  means a time-domain signal obtained as an output of system  $G(s)$  using  $u(t)$  as the input signal [17], and  $\theta(t)$  represents input current  $I$  of fuel cell and  $y(t)$  represents the output power  $P$ . Therefore,

$$\begin{aligned} \tilde{\theta} &= \theta^* - \frac{k}{s^\alpha} [b \sin(\omega t) \frac{s^\beta}{s^\beta + \omega_h} [P]] \\ &= \theta^* - \frac{k}{s^\alpha} [b \sin(\omega t) \frac{s^\beta}{s^\beta + \omega_h} [f^* + (\theta - \theta^*)^2]] \end{aligned} \quad (14)$$

$$\tilde{\theta} + \frac{2kab}{s^\alpha} [\sin(\omega t) \frac{s^\beta}{s^\beta + \omega_h} [\tilde{\theta} \sin(\omega t)]] = \theta^* + \varepsilon \quad (15)$$

where  $\varepsilon$  is the dynamic response part attenuating to zero.

### C. ESC With Fractional Order Integrator

Considering the case of a fractional order integrator working with an integer order HPF in ESC, which means  $1/s^\alpha$  ( $0 < \alpha < 1$ ) is adopted as an integrator, the transfer function is:

$$\begin{aligned} \frac{\tilde{\theta}}{\theta^*} &= \frac{1}{1+L(s)} \\ &= \frac{s^\alpha (s^2 + 2\omega_h s + \omega_h^2 + \omega^2)}{s^{\alpha+2} + kab s^2 + 2\omega_h s^{\alpha+1} + (\omega_h^2 + \omega^2) s^\alpha + kab \omega_h s + kab \omega^2}. \end{aligned} \quad (16)$$

And the roots of the characteristic equation determine this ESC system's stability.

$$D(s) = s^{\alpha+2} + kab s^2 + 2\omega_h s^{\alpha+1} + (\omega_h^2 + \omega^2) s^\alpha + kab \omega_h s + kab \omega^2 = 0. \quad (17)$$

### D. ESC With Fractional Order HPF (FO-HPF)

Considering the case of a FO-HPF working with an integer order integrator in ESC, here, the FO-HPF is defined as

$$G_{\text{FO-HPF}}(s) = \frac{s^\beta}{s^\beta + \omega_h}, \quad 0 < \beta < 1 \quad (18)$$

Finally, the transfer function can be obtained as

$$\begin{aligned} \frac{\tilde{\theta}}{\theta^*} &= \frac{1}{1+L(s)} \\ &= \frac{s(s^{2\beta} + 2\omega_h s^{2\beta} + \omega_h^2 + \omega^2)}{s(s^{2\beta} + 2\omega_h s^\beta + \omega_h^2 + \omega^2) + kab(s^{2\beta} + 2\omega_h s^\beta + \omega_h^2 + \omega^2)}. \end{aligned} \quad (19)$$

### E. Approximation of Fractional Order Integrator $1/s^\alpha$

Since FO-HPF can be represented as a closed-loop with fractional order integrator as shown in Fig. 7, therefore, the main calculation in the situation of fractional order integrator and FO-HPF is related to the approximation of fractional order integrator  $1/s^\alpha$  with integer order rational polynomial. The MATLAB Toolbox Ninteger [19] is chosen to approximate the fractional order integrator  $1/s^\alpha$ .

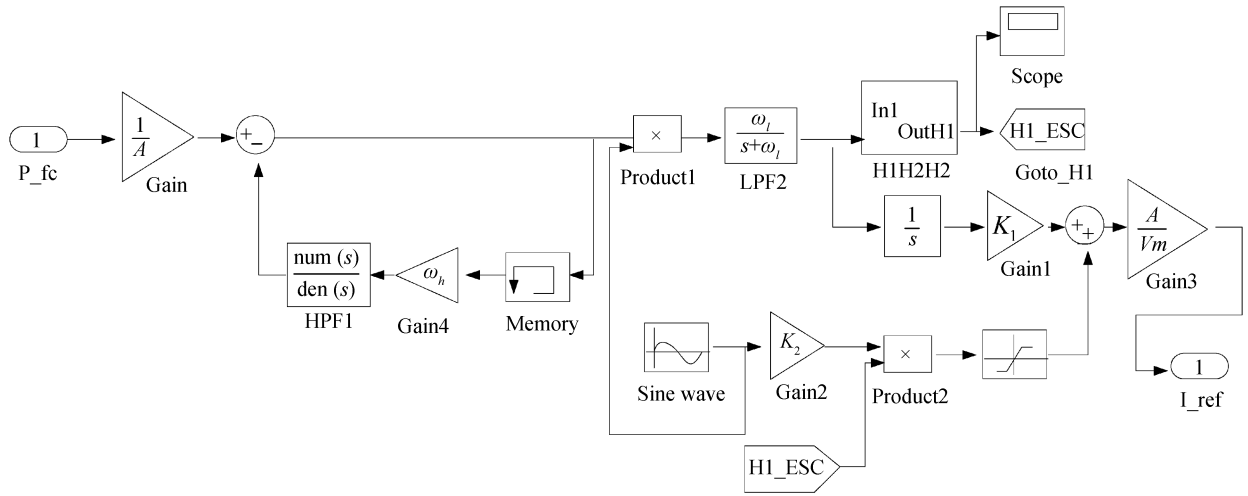


Fig. 7. MPPT controller with FO-HPF in Simulink.

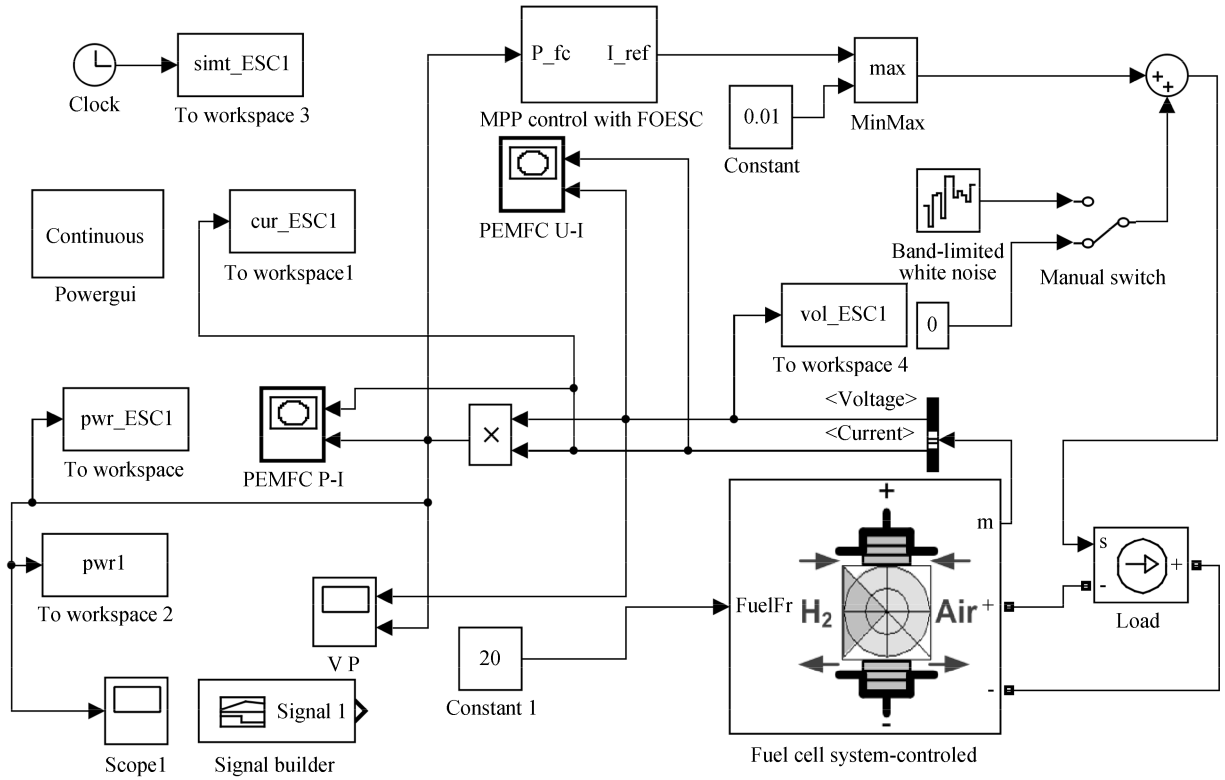


Fig. 8. Fuel cell with MPPT controller in Simulink.

#### IV. SIMULATION RESULTS AND DISCUSSIONS

The focus of this paper is to discuss the role of fractional order controller in ESC. Here, the fuel cell model in MATLAB/Simulink as shown in Fig. 8 is adopted. The fuel cell model is a 6 kW & 45 V PEMFC stack from the SimPowerSystem Toolbox in MATLAB, which is fueled with hydrogen (FuelFr value) and air at nominal flow rate of 50 lpm (liters per minute) and 300 lpm, respectively. As a comparison, the model in [20] is used as the reference. The simulation models of the ESC controller with FO-HPF used in Simulink are shown in Fig. 4. The MPP here for comparison relates to the case when the FuelFr value is given as 20 lpm, without loss of generality. Some key parameters are given in Table I.

TABLE I  
SIMULATION PARAMETERS

Parameters	Formula	Value
Frequency $f_1$ (Hz)		100
Cutoff radian frequency of HPF $\omega_h$		62.8
Perturbation radian frequency		628
Activation area $A$ ( $\text{cm}^2$ )		56
Loop gain $K_1$	$4 * f_1$	400
Sine gain $K_2$		10
$V_m$		45
Gain $k$	$K_1/V_m$	8.9
Magnitude $a$		1
Magnitude $b$	$K_2 * H_1 * A/V_m$	$12.4 * H_1$

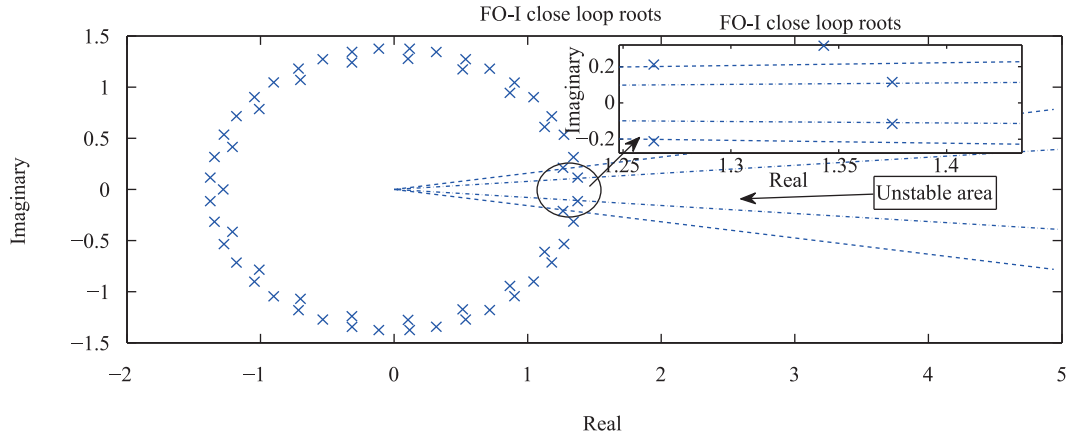


Fig. 9. Root map of ESC with fractional order integrator.

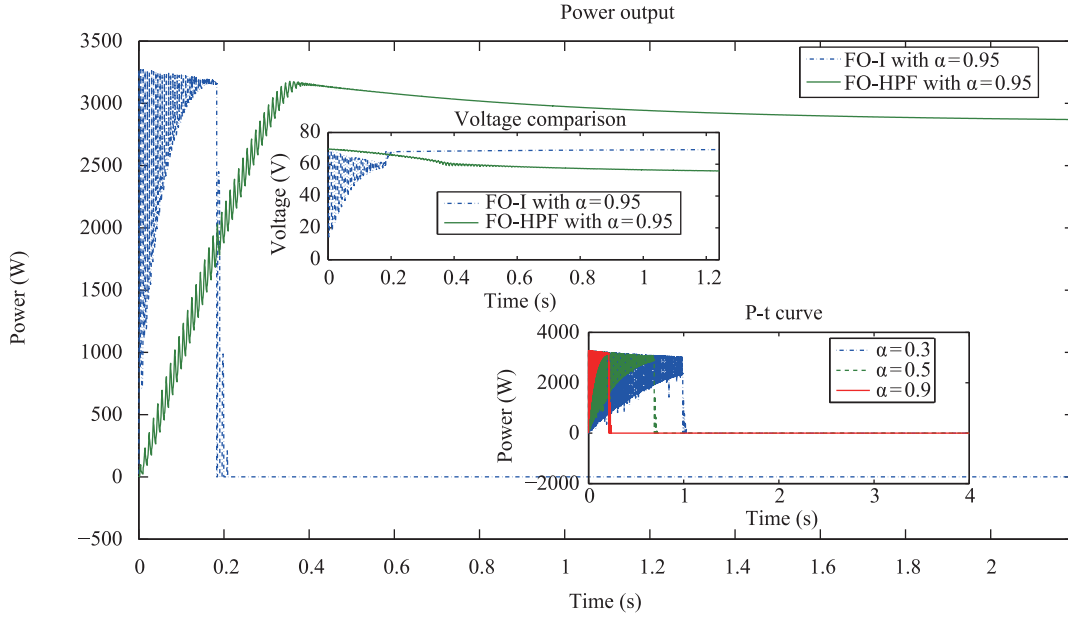


Fig. 10. Power/voltage output using ESC with fractional order integrator.

#### A. Performance of ESC Using Fractional Order Integrator With Order $\alpha$

During simulation, when  $\alpha$  varies between 0.3 and 1, the tracking of the MPP fails and when  $\alpha$  is less than 0.3, no simulation result can be gained, showing that the tracking process is nonconvergent and the system is unstable. So, it is necessary to explain why this phenomenon occurs. Taking  $\alpha = 0.95$  as an example, the characteristic polynomial is:

$$D(s) = s^{\frac{59}{20}} + c_1 s^{\frac{40}{20}} + c_2 s^{\frac{39}{20}} + c_3 s^{\frac{20}{20}} + c_4 s^{\frac{19}{20}} + c_5. \quad (20)$$

This is a commensurate-order system, and the closed-loop root map in the  $\lambda = s^{1/20}$  plane is shown in Fig. 9. It can be found that there are two roots  $1.375 \pm j0.115$  with angle of 0.0785 radians very close to the stability boundary angle of  $1/20(\pi/2)$ . So, the stability condition is very poor which leads to the abnormal voltage output, and it fails to track the MPP, as shown in Fig. 10. This phenomenon also exists in other cases using different order  $0.3 < \alpha < 1$ .

#### B. Performance of ESC Using FO-HPF With Order $\beta$

The characteristic polynomial is:

$$D(s) = s(s^{2\beta} + 2\omega_h s^\beta + \omega_h^2 + \omega^2) + kab(s^{2\beta} + 2\omega_h s^\beta + \omega_h^2 + \omega^2). \quad (21)$$

Given  $\beta = 0.95$ ,

$$D(s) = s^{\frac{58}{20}} + d_1 s^{\frac{39}{20}} + d_2 s^{\frac{38}{20}} + d_3 s^{\frac{20}{20}} + d_4 s^{\frac{19}{20}} + d_5. \quad (22)$$

This is also a commensurate-order system, and the closed-loop root map in the  $\lambda = s^{1/20}$  plane is shown in Fig. 11. It can be found that there are roots  $1.398 \pm j0.128$  with angle of 0.091 radian which is less close to the critical stable boundary angle of  $1/20(\pi/2)$  than the case using fractional order integrator, which means FO-HPF improves the tracking stability. And the power vs. time curves under different fractional orders are shown in Fig. 12. It can also be found that the larger the fractional order  $\alpha$  the faster the power responses, but the integer-order HPF has the fastest response speed.

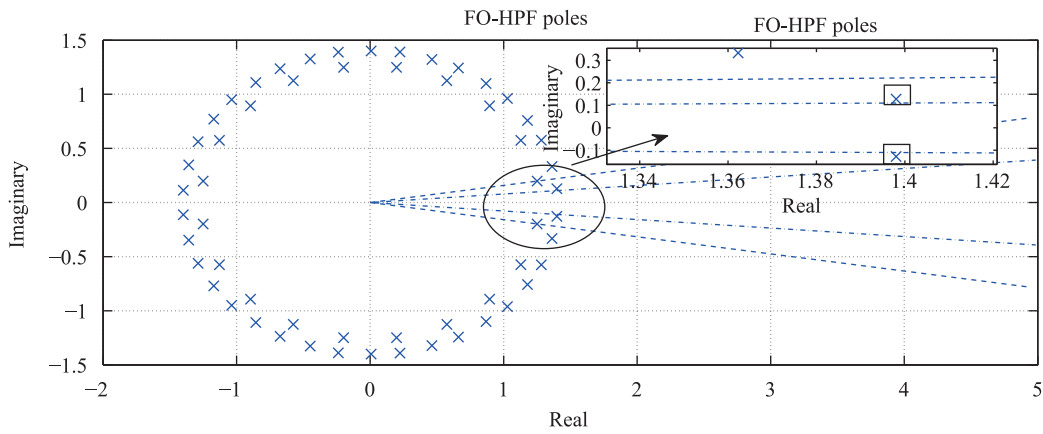


Fig. 11. Root map of FO-HPF-ESC.

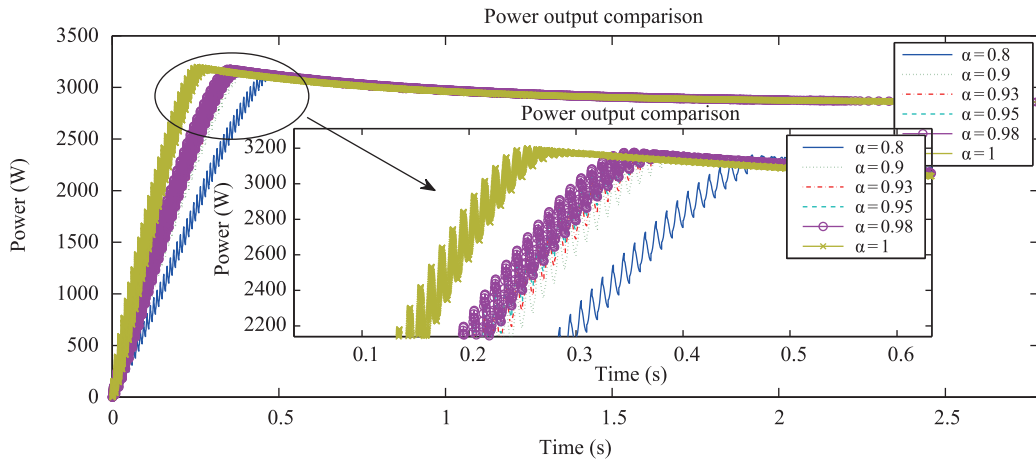


Fig. 12. Power output with FO-HPF-ESC.

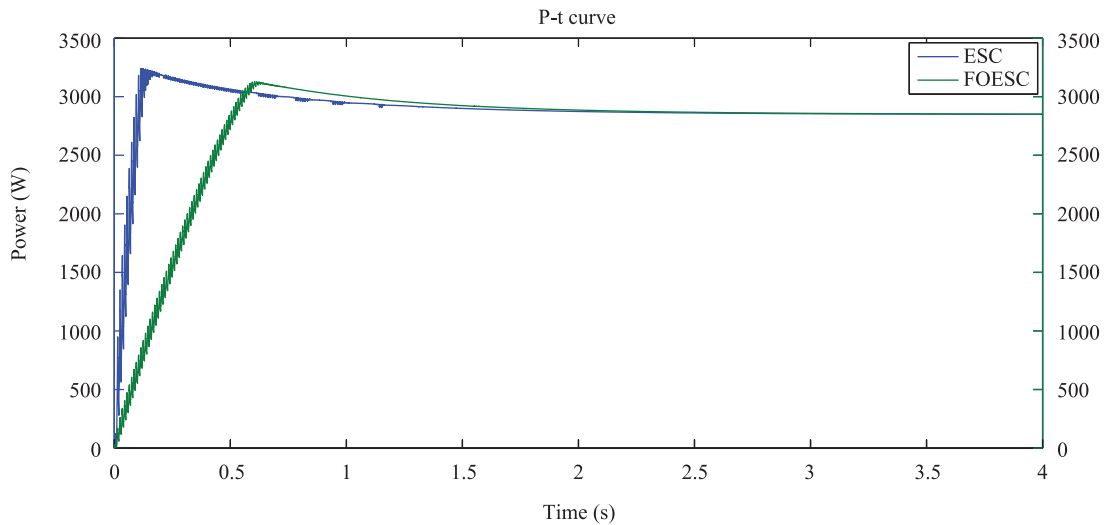


Fig. 13. Power-time curve comparison.

C. Performance of ESC Using FO-HPF With LPF

The ESC controller using fractional high-pass filter, together with integer-order integrator and integer-order low-pass filter, has the structure shown in Fig. 7.

1) Power Output Comparison

As shown in Fig. 13, the fuel cell controlled by an integer-order ESC, which uses dither amplitude proportional to the magnitude of the first harmonics of the processed FC power,

has faster response speed than the one using FO-HPF ESC and marked with green color.

2) Attraction Range of MPPT

When the fuel input is 20 lpm, as an example, the relationship between the fuel cell power output and the current is shown in Fig. 14. It is obvious that the current fluctuation when using the FO-HPF ESC (green one) during tracking is smaller near the maximum power point, with range 52–53, comparing to 51–57 of the regular ESC method.

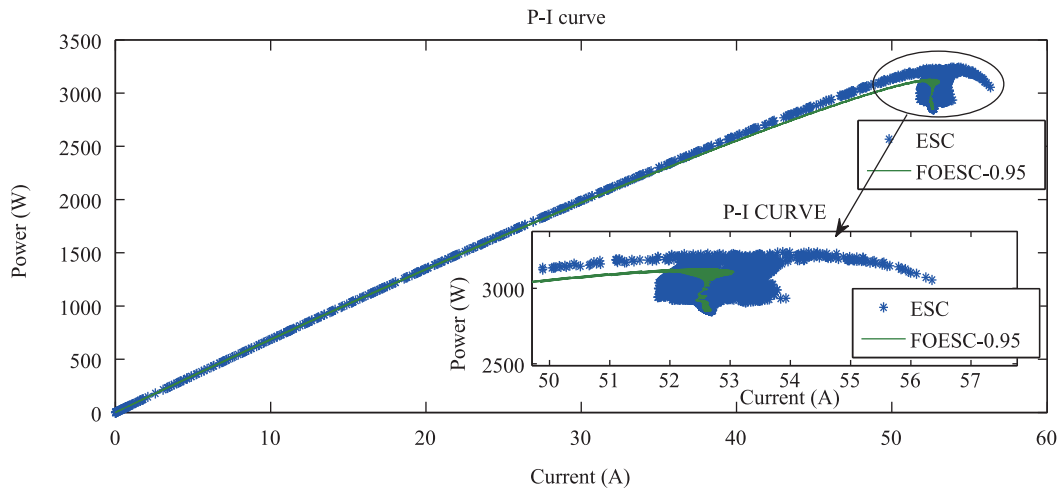
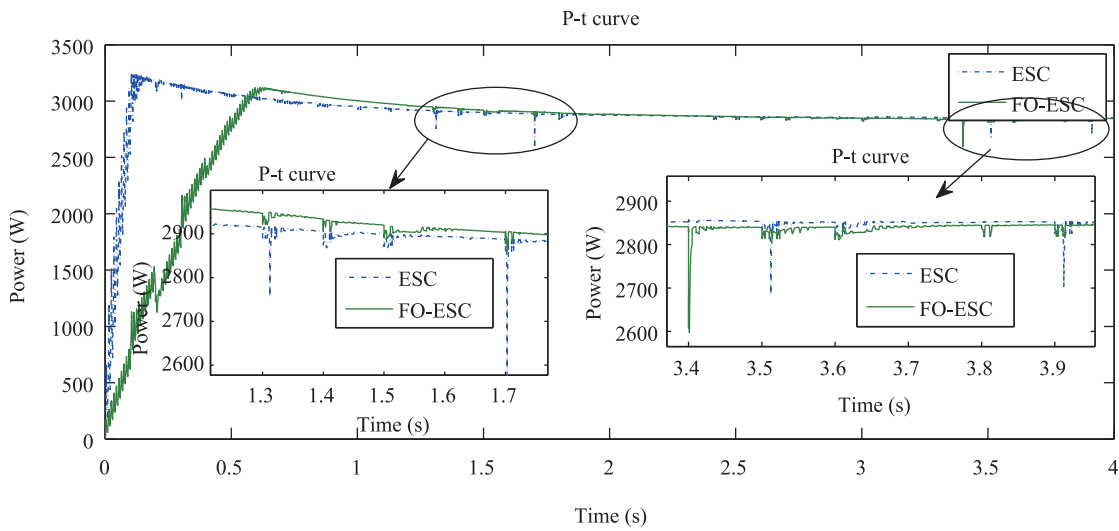
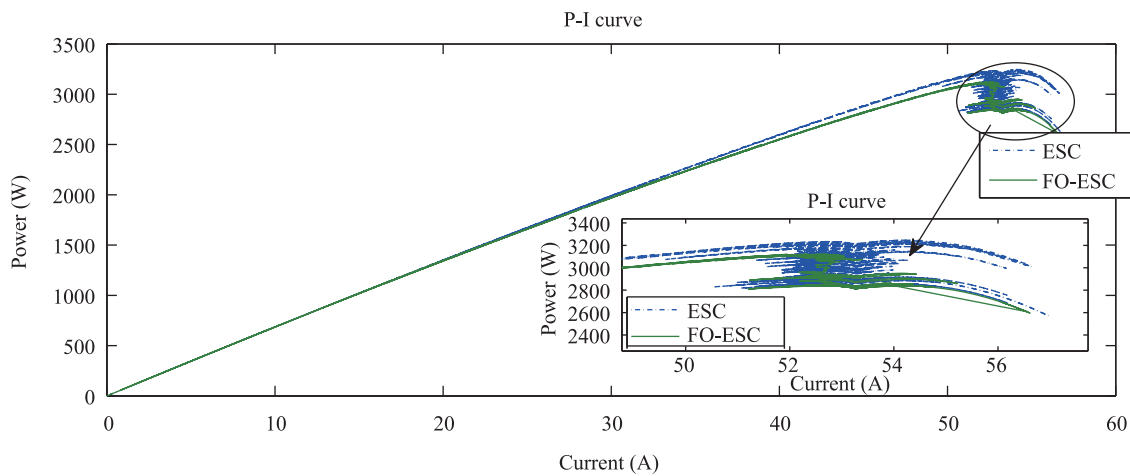


Fig. 14. Power output vs current during tracking.



(a) Power-time curve comparison ESC



(b) Power-current curve comparison

Fig. 15. MPPT performance under white noise.

3) Robustness Under White Noise

If band-limited white noise with power of 0.04 is applied, fuel cell power outputs are shown in Fig. 15. It is obvious

that the tracking process with FO-HPF (the blue curve) outperforms the one using normal HPF. Fig. 16 shows the MPPT when the load varies in the case of Fig. 17. So, FO-HPF-ESC offers more stable tracking ability than the usual ESC.

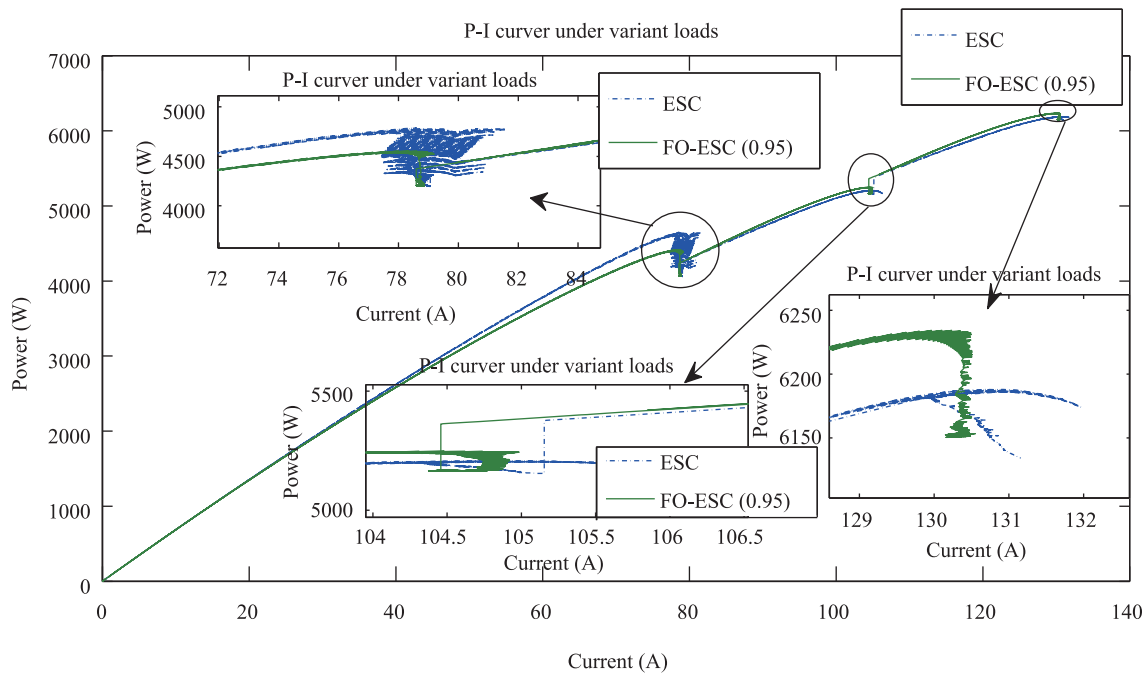


Fig. 16. MPPT performance under variant loads.

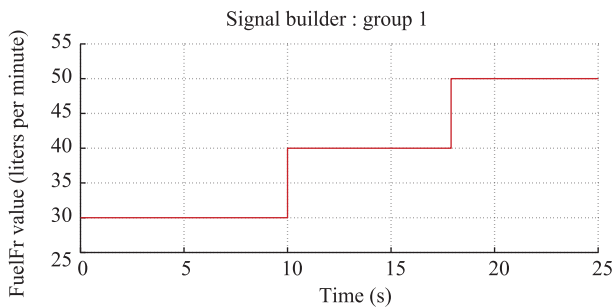


Fig. 17. Variant loads.

## V. CONCLUSIONS

In this paper, a novel ESC algorithm is presented which is an ESC with FO-HPF. As discussed in this paper, separate fractional order integrator may cause the tracking failure because of the poor tracking stability, and using FO-HPF in the ESC structure reduces the dynamic response fluctuation. In addition, FO-HPF-ESC increases the robustness compared to the regular ESC. As can be seen in our simulation results, FO-HPF-ESC not only can follow the maximum power point smoother than the regular ESC, but also shows more robustness in the presence of disturbance in the system. However, for the given application case, only adjusting the order of FO-HPF is difficult to improve the response speed. Furthermore, how to optimize the order of FO-HPF instead of trial-and-error is still open and worthy of intensive research.

## ACKNOWLEDGEMENTS

The authors would like to thank Prof. Nicu Bizon at the University of Pitesti, Romania and Prof. WoonKi Na at the

California State University, Fresno, USA, and Dr. Hadi Malek, for their help and valuable advices in this work.

## REFERENCES

- [1] X. P. Zhou, S. Yuan, C. Wu, B. Song, and S. L. Peng, "Potential production and distribution of microalgae in China," *J. Renew. Sustain. Energ.*, vol. 5, no. 5, pp. 053101, 2013.
- [2] H. B. Khalil and S. J. H. Zaidi, "Energy crisis and potential of solar energy in Pakistan," *Renew. Sustain. Energ. Rev.*, vol. 31, pp. 194–201, Mar. 2014.
- [3] J.-M. Chevalier, *The New Energy Crisis: Climate, Economics and Geopolitics*. London: Palgrave Macmillan, 2009.
- [4] A. Rashid, K. Yousaf, S. Shah, and N. Shaukat, "Electricity crisis and the significance of indigenous coal for electric power generation," *Electronic Devic.*, vol. 4, no. 1, pp. 1–11, Mar. 2015.
- [5] A. Omri and A. Chaibi, "Nuclear energy, renewable energy, and economic growth in developed and developing countries: a modelling analysis from simultaneous-equation models," Technical Report, Department of Research, IPAG Business School, Paris, 2014.
- [6] O. Z. Sharaf and M. F. Orhan, "An overview of fuel cell technology: fundamentals and applications," *Renew. Sustain. Energ. Rev.*, vol. 32, pp. 810–853, Apr. 2014.
- [7] J. Larminie and A. Dicks, *Fuel cell systems explained* (Second edition). New York: Wiley, 2003.
- [8] K. N. Mobariz, A. M. Youssef, and M. Abdel-Rahman, "Long endurance hybrid fuel cell-battery powered UAV," *World J. Modell. Simul.*, vol. 11, no. 1, pp. 69–80, 2015.
- [9] Z. D. Zhong, H. B. Huo, X. J. Zhu, G. Y. Cao, and Y. Ren, "Adaptive maximum power point tracking control of fuel cell power plants," *J. Power Sourc.*, vol. 176, no. 1, pp. 259–269, Jan. 2008.

- [10] N. Karami, R. Outbib, and N. Moubayed, "Maximum power point tracking with reactant flow optimization of proton exchange membrane fuel cell," *J. Fuel Cell Sci. Technol.*, vol. 10, no. 5, pp. 051008, Aug. 2013.
- [11] D. P. Hohm and M. E. Ropp, "Comparative study of maximum power point tracking algorithms," *Progr. Photovolt.: Res. Applic.*, vol. 11, no. 1, pp. 47–62, Jan. 2003.
- [12] M. Krstić and H.-H. Wang, "Stability of extremum seeking feedback for general nonlinear dynamic systems," *Automatica*, vol. 36, no. 4, pp. 595–601, Apr. 2000.
- [13] C. Yin, B. Stark, Y. Q. Chen, and S. M. Zhong, "Adaptive minimum energy cognitive lighting control: integer order vs fractional order strategies in sliding mode based extremum seeking," *Mechatronics*, vol. 23, no. 7, pp. 863–872, Oct. 2013.
- [14] C. Yin, Y. Q. Chen, and S. M. Zhong, "Fractional-order sliding mode based extremum seeking control of a class of nonlinear systems," *Automatica*, vol. 50, no. 12, pp. 3173–3181, Dec. 2014.
- [15] N. Bizon, "FC energy harvesting using the MPP tracking based on advanced extremum seeking control," *Int. J. Hydrogen Energ.*, vol. 38, no. 4, pp. 1952–1966, Feb. 2013.
- [16] M. Dargahi, J. Rouhi, M. Rezanejad, and M. Shakeri, "Maximum power point tracking for fuel cell in fuel cell/battery hybrid power systems," *Eur. J. Sci. Res.*, vol. 25, no. 4, pp. 538–548, Jan. 2009.
- [17] M. Krstić, "Performance improvement and limitations in extremum seeking control," *Syst. Contr. Lett.*, vol. 39, no. 5, pp. 313–326, Apr. 2000.
- [18] H. Malek, "Control of grid-connected photovoltaic systems using fractional order operators," Ph. D. dissertation, Utah State University, Logan, Utah, 2014.
- [19] D. Valério, "Toolbox Ninteger for MATLAB, v. 2.3 (September 2005)," 2015. [Online]. Available: <http://web.ist.utl.pt/duarte.valerio/ninteger/ninteger.htm>
- [20] N. Bizon, "On tracking robustness in adaptive extremum seeking control of the fuel cell power plants," *Appl. Energ.*, vol. 87, no. 10, pp. 3115–3130, Oct. 2010.



**Jianxin Liu** graduated from Wuhan Iron and Steel University (WISU), China, in 1991. He received the M.E. degree from WISU in 1994 and the Ph.D. degree from the Chongqing University, China, in 1997. He is currently a professor at the School of Mechanical Engineering, Xihua University, China. His research interests include robotics and automation, especially the control of robots such as visual servoing control and intelligent control. Corresponding author of this paper.



**Tiebiao Zhao** graduated from Yantai University, China, 2009. He received his M.Sc. degree in control theory and control engineering from University of Science and Technology of China, China, 2012. Currently he is the third year Ph.D. candidate in University of California, Merced. His research interests include applications of small unmanned aerial systems (sUAS) in precision agriculture, especially water stress detection and yield prediction.



**YangQuan Chen** received his Ph.D. degree in advanced control and instrumentation from Nanyang Technological University, Singapore, in 1998. Dr. Chen was on the Faculty of Electrical and Computer Engineering at Utah State University before he joined the School of Engineering, University of California, Merced in 2012 where he teaches mechatronics for juniors and fractional order mechanics for graduates. His current research interests include mechatronics for sustainability, cognitive process control and hybrid lighting control, multi-UAV based cooperative multi-spectral personal remote sensing and applications, applied fractional calculus in controls, signal processing and energy informatics; distributed measurement and distributed control of distributed parameter systems using mobile actuator and sensor networks.